Proceedings of the 2005 IEEE
International Conference on Robotics and Biomimetics
June 29 - July 3, 2005, Hong Kong and Macau

Automating Micro Cellular Detection Process Using All-Transparent Microfluidic Platform and Surface Plasmon Resonance Technique

Kin Fong Lei[1], Wing Cheung Law[2], Chi Lok Wong[2], Wen J. Li[1,*], Ho Pui Ho[2,#], Siu-Kai Kong[3,+], and Chinlon Lin[2]

[1]Centre for Micro and Nano Systems
Faculty of Engineering

[2]Center for Advanced Research in Photonics
Faculty of Engineering

[3]Department of Biochemistry
Faculty of Science

The Chinese University of Hong Kong, Hong Kong SAR

[*]Contact Author: wen@acae.cuhk.edu.hk

Abstract - **This paper reports an automated polymer based microfluidic analysis system integrated with the surface plasmon resonance (SPR) biosensor for qualitatively monitoring of cell adhesion on the sensor surface. Micropumps, microchannels, and SPR biosensor were integrated into a single polymer (PMMA) based microfluidic system. The integrated system has been studied in its potential application in drugs discovery. An experiment, which is monitoring the activities of living cells in the presence or absence of trypsin in RPMI-1640 medium, was conducted to show the ability of its biomedical application. Because SPR based bio-detection requires optically transparent substrates, PMMA is a potential replacement for glass and silicon-glass in microfluidic systems, if bio-compatibility and low-cost are desired. Hence, our work has shown the feasibility of commercializing SPR based biomedical/chemical analyses system in the near future. Furthermore, an advanced 2-dimensional multi-chamber microfluidic system with the SPR imaging detection system for detecting the specific binding of biomolecules was also conduced. It shows the possibility of the parallel detection process.**

Index Terms – **Microfluidic System, SPR Sensor, Cellular Detection.**

I. INTRODUCTION

The research on microfluidics involves the development of miniaturized devices, miniaturized systems, and applications related to the handling of fluids. Over the past ten years, microfluidic lab-on-chip system has been rapidly developed from early single channel devices [1] to current complex analysis systems [2]. The rapid growth of this field is partly due to the rapid developments in MEMS devices, such as micropumps, micromixers, and biosensors, as well as the need for high throughput biomedical analysis and drug delivery system. New generations of automated microfluidic devices have made it possible to achieve biomedical instruments with new levels of performance and capability. Moreover, in the area of biosensors, surface plasmon resonance (SPR) has become a leading technology in biological and chemical sensing because of its real-time and label-free detection capabilities for bio-molecules [3]. Recently, we have proposed a new SPR biosensor design based on measuring the differential optical phase between the *s* and *p* polarizations [4]. The new technique offers a better sensitivity because of its effectiveness in minimizing common-mode noise through the use of differential measurement.

In this paper, a fully automated microfluidic system integrated with a phase-sensitive SPR biosensor is presented. The system consists of three vortex micropumps [5] and a SPR biosensor head [4]. The entire microfluidic system can be fabricated using a low-cost micro molding replication technique. The working principal of the vortex micropump is based on the vortex flow generation inside the pump chamber by an SU-8 fabricated micro impeller. From our pervious experiments, the vortex micropump can generate a flow rate from 0.11 to 9.5ml/min at an applied voltage from 0.6 to 2.5V with linear relationship. Integrating three vortex micropumps and a SPR biosensor into a single chip, an automated fluid manipulation and bio-detection system can be achieved. The micropumps are software-controlled to pump different solutions sequentially into the SPR biosensor head. For the SPR sensor, results from our pervious work [4] using glycerin-water mixtures indicate that the sensitivity limit of our design can be as high as 5.5×10^{-8} refractive-index units. Such an improvement in the sensitivity limit should put SPR biosensors as a possible replacement of conventional biosensing techniques that are based on fluorescence. We have used our experimental setup, which has real-time phase extraction and software control capabilities, to perform an experiment, monitoring cell adhesion properties under the influence of trypsin.

II. EXPERIMENTAL SETUP

2.1. Surface Plasmon Resonance

A prism-coupled Kretschmann scheme depicted in Fig. 1 is often used in SPR sensor system. The surface

[*]For questions pertaining to microfluidic transport automation: wen@acae.cuhk.edu.hk; [#]for questions pertaining to SPR detection: hpho@ee.cuhk.edu.hk; [+]for questions pertaining to bio-molecule and cellular analyses: skkong@cuhk.edu.hk. This project is funded by the Hong Kong Research Grants Council (No. CUHK 4215/01E) and by a CUHK Direct Grant (No.2050305). Wen J. Li is an associate professor at The Chinese University of Hong Kong and also a Distinguished Overseas Scholar of the Chinese Academy of Sciences. Partial support is also provided by the Shenyang Institute of Automation, Chinese Academy of Sciences.

0-7803-9315-5/05/$20.00 ©2005 IEEE

plasmon wave (SPW) vector (k_{sp}) between the metal and dielectric medium can be expressed as:

$$k_{sp} = k_o \sqrt{\frac{\varepsilon_{metal}\varepsilon_{sample}}{\varepsilon_{metal} + \varepsilon_{sample}}} \quad (1)$$

where k_o is the free space wave vector of the optical wave, ε_{metal} and ε_{sample} are the complex dielectric constants of the metal and the sample medium respectively. The enhanced wave vector of incident light (k_x) is given by:

$$k_x = k_o n_{glass} \sin\theta_{inc} \quad (2)$$

where n_{glass} is the refractive index of the prism, θ_{inc} the angle of incidence. For SPR to take place, which leads to the strongest SPW, the two vectors should be matched. i.e.

$$k_x = k_{sp} \quad (3)$$

The simplest way to express the phase property of SPR is to use Fresnel equation, the reflection coefficients of the *p*- and *s*-polarized light (r_p and r_s), which are given by [7]:

$$r_p = |r_p| e^{i\phi_p} \text{ and } r_s = |r_s| e^{i\phi_s} \quad (4)$$

Across the resonant peak, the phase angle will exhibit a steep change, which means that a small variation of ε_{sample} or refractive index of sample will lead to a large phase change in the reflected light. Due to the fact that SPR effect will only affect *p*-polarized light, the value of phase different ($\Delta\phi$) between *p*-polarization and *s*-polarization ($\phi_p - \phi_s$) can be used as a refractive index probe on the sensor surface (for detailed explanation, see ref [4]).

2.2. Vortex micropump

In our automated microfluidic system, fluid flow is driven by vortex micropumps. Detailed fabrication and modeling results developed by our group have been presented in ref [5][6]. The vortex micropump uses kinetic energy to move fluid through the use of an impeller and a circular pump chamber. The basic design concept is illustrated in Fig. 2. As fluid enters the pump near the center of the impeller, it is moved towards the outer diameter of the pump chamber by the rotating motion of the impeller. The confinement provided by the

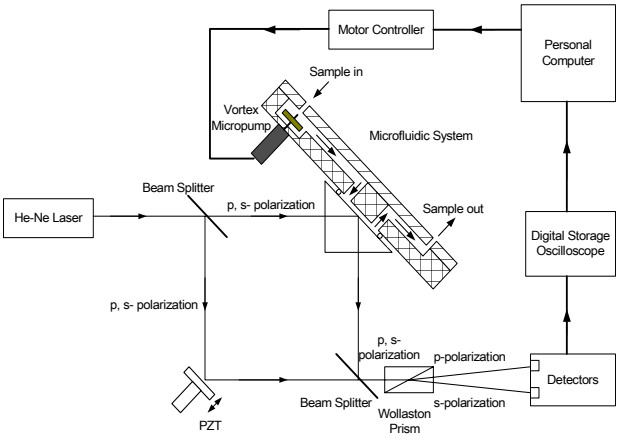

Fig. 1. Experimental setup of the microfluidic system integrated with the SPR biosensor.

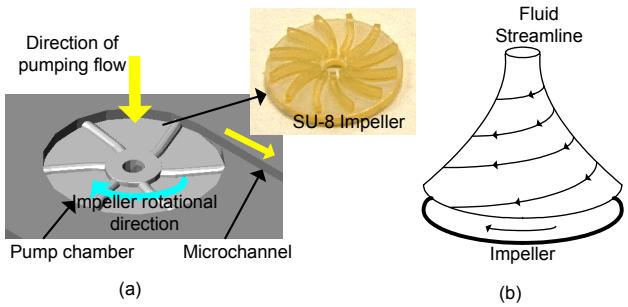

Fig. 2. (a) Illustration of the vortex micropump working principle. (b) Fluid streamline inside the pump chamber.

pump chamber forces the fluid to enter the microchannel and a pumping flow is thus created. Since the generation of pumping flow is due to the rotating motion of the impeller, the pumping flow rate can be controlled smoothly by changing the rotational speed of the impeller. This allows digitally controlled fluidic manipulation through straightforward control software.

As mentioned earlier, microfluidic systems are required to be optically transparent and bio-compatible for bio-optical detection and chemical applications. For our vortex micropump, we choose polymethyl methacrylate (PMMA) to be the structural material. The SU-8 micro impeller is placed inside the pump chamber. When the fluid enters the micropump from the center of impeller, the rotational motion of impeller, driven by a DC motor, can induce a fluid pressure gradient and thus create a continuous flow. In our vortex pump design, two structural layers are needed. The lower layer includes pump chamber and microchannel, while the upper layer is a cover layer providing fluidic connection. A completed vortex micropump with microchannel is shown in Fig. 3. The diameter of pump chamber is 5mm. The fluid is pumped through an output microchannel of 300μm in width and 200μm in depth.

Experimental and simulation results on the flow rate and pump pressure as a function of rotational speed of the impeller are shown in Fig. 4. The pump performance of two different sizes of the pump chamber, which are 3mm and 5mm in diameter, feeding identical output microchannels are also compared. Our results confirm that the fluid flow rate and pump pressure are proportional to the impeller rotational speed. This also means that the flow rate and pump pressure increase linearly with the DC voltage applied to the motor. From the comparison between two different pump chamber sizes, we found that the larger pump chamber can produce higher fluid flow rate and pressure level. Our experimental data shows that the minimum pump rate and pump pressure are 0.11ml/min and 166Pa at the startup voltage (0.75V) of the DC motor, respectively. The maximum flow rate and pump pressure are 9.5ml/min and 8000Pa at the applied voltage of 2.5V. We have derived an analytical model to approximate the vortex pump performance using the Hagen-Poiseuille equations [6]. The simulation results are compared to experimental results in Fig. 4.

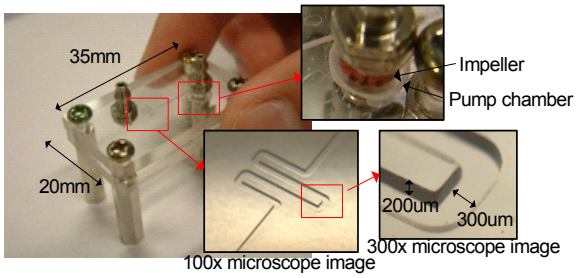

Fig. 3. Photo of a vortex micropump with microchannel. The chip size is 20mm × 35mm. The diameter of pump chamber is 5mm. The output microchannel is 300μm in width, 200μm in depth.

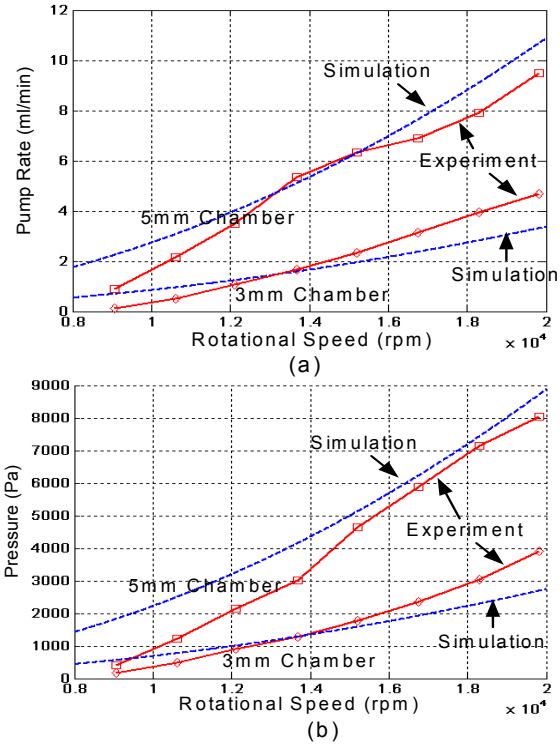

Fig. 4. Comparison of the experimental (solid line) and simulation (dotted line) results. (a) Comparison of pump rate (water as pump medium) as a function of rotational speed of impeller at zero back pressure. (b) Comparison of pumping pressure (water as pump medium) as a function of rotational speed of impeller at zero flow rate.

2.3 Integrated microfluidic system

The experimental setup of the microfluidic system is illustrated in Fig. 1. Three vortex micropumps and a SPR biosensor are integrated into a polymer-based single chip with a computer to control the flow sequence and analyse the SPR signals in a real time manner. In this setup, three different solutions can be pumped into the SPR biosensor head independently. A Mach-Zehnder interferometer with a 10mW polarized He-Ne laser operating at 632.8nm is used as the light source. The polarization direction of the output beam is tuned at 30°

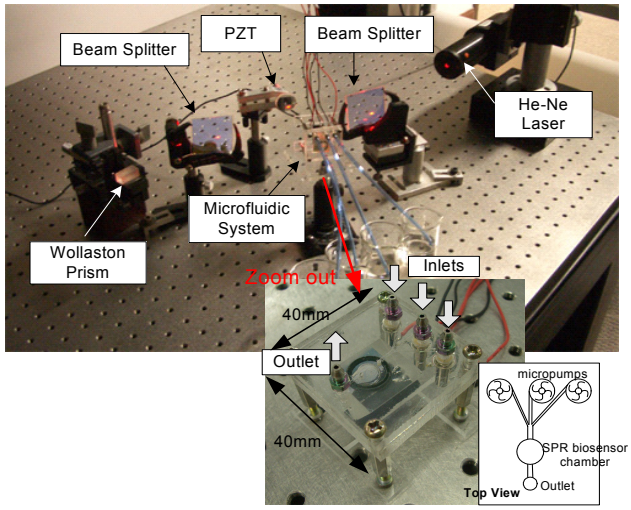

Fig. 5. Experimental setup of the automated microfluidic system integrated with the SPR biosensor for micro cellular detection. (zoom out) A photo of the polymer based microfluidic system integrated with SPR biosensor. The size of the whole chip is 40mm x 40mm. There are three independent inlets for three different solutions.

from *p*-polarization so that a larger amount of light intensity can be contributed to *p*-polarization to enhance the signal-to-noise ratio of the probe beam. For the sensor head, we use a nominally 45nm gold-coated glass plate attached to a 60° equilateral prism made from BASF10 glass using matching oil. The first 50:50 beam splitter divides the laser into two halves. One beam (probe beam) goes to the sensor head while the beam (reference beam) goes to the plane mirror. A piezoelectric transducer (PZT) is attached to the back of the mirror and a saw-tooth wave oscillating at 120Hz is used to provide the phase modulation signal required by the phase measurement software. Constructive and destructive interferences occurred periodically as a time-varying path difference are introduced by the back-and-forth movement of the mirror. The probe beam and reference beam are combined again at the second beam splitter. In the output beam *p*- and *s*-polarization light are separated by the use of Wollaston prism. Two detectors together with a digital oscilloscope are used to capture the signal and finally the differential phase quantity is extracted. Our experimental setup and the microfluidic system are shown in Fig. 5.

III. MICRO CELLULAR DETECTION

3.1 Material

The cells that we used in our experiment were mouse L929 cell (4 x 10^6 cells/ml) obtained from ATCC (American Type Culture Collection). Prior to the experiment, the mouse cells were put in a rich nutrition buffer, RPMI Medium 1640 from Invitrogen Corporation. RPMI (Roswell Park Memorial Institute) Medium 1640 are liquid medium with enriched formulations for culturing living mammalian cells [8]. With the aid of RPMI, living L929 cells will naturally attach to the gold

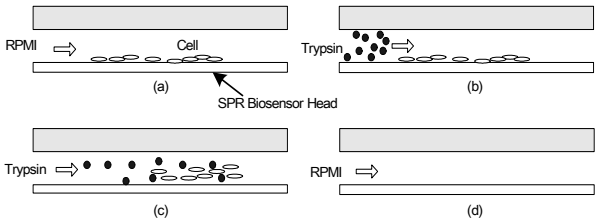

Fig. 6. Illustration of detecting of cell detachment. (a) Injection of RPMI. (b) Injection of trypsin. (c) Detaching cell from the sensor head. (d) No cell left on the sensor surface.

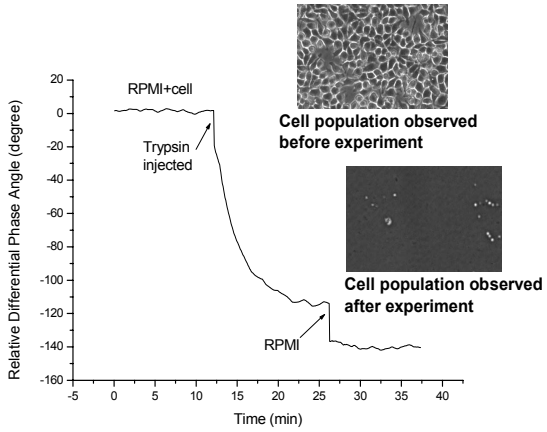

Fig. 7. Differential phase response curve due to sequential addition of RPMI containing cells, trypsin, and RPMI into sensor head.

surface. Trypsin-EDTA (0.25% Trypsin) obtained from Invitrogen Corporation is a common reagent used to remove and detach cells from culture substratum. Trypsin was thus used in our experiment to detach the cells from the gold surface by breaking the adhesion proteins between the cell and the gold surface.

3.2 Results

The process sequence is illustrated in Fig. 6. Mouse L929 cells (4 x 10^6 cells/ml) were first cultured on a 45nm gold-coated glass plate at 37°C for two hours. Then the gold surface was observed under an optical microscope to ensure cells were well adhered to the glass plate. As shown in the in-set of Fig. 7, cells were adhered on the gold surface as a monolayer. This glass plate was then attached to a prism using matching oil for phase-sensitive SPR bio-sensing studies. RPMI Medium 1640 was first flowed into the chamber to measure differential phase as a baseline. Trypsin-EDTA (0.25% Trypsin) was then injected into the sensor head. As shown in Fig. 7, an exponential decay curve was observed indicating that the cells were detached from the gold surface. Finally, RPMI was circulated to ensure all the cells were suspended. Another set of control experiment was carried out by repeating the experiment with bare gold glass plate. A small phase angle changed was observed when trypsin is added. Thus, we conclude that the large phase change observed in Fig. 7 must be largely caused by cells detachment. At the end of the experiment, the glass plate

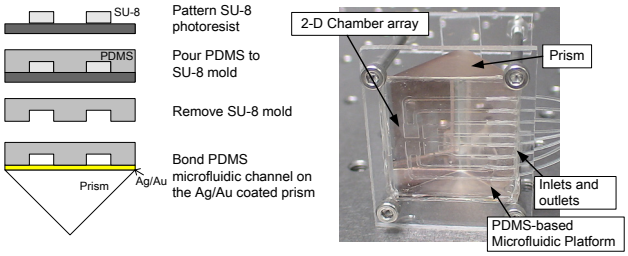

Fig. 8. (left) Fabrication process of PDMS-based microfluidic platform. (right) Photo of PDMS-based microfluidic platform. There are four independent flow chambers.

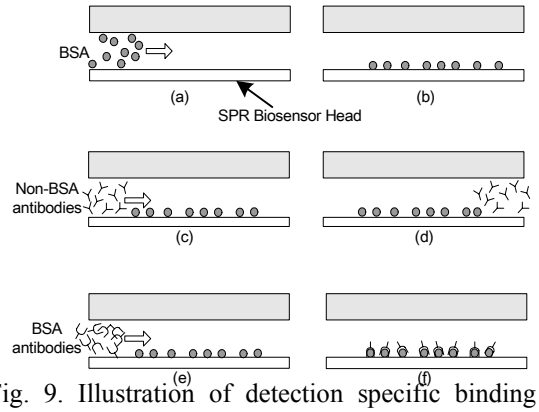

Fig. 9. Illustration of detection specific binding of antibodies. (a) Injection of BSA. (b) Forming of a layer of BSA on the sensor head. (c) Injection of nonspecific BSA antibodies (Rat IgG). (d) Removal of non-specific antibodies without any binding. (e) Injection of specific BSA antibodies. (f) Specific binding of BSA to BSA antibodies.

was taken out from the prism and observed again under an optical microscope. Visual inspection confirmed that almost all the cells were removed from the surface. Our results show that one can monitor cell detachment affinities using SPR. This is a very useful platform for a range of biomedical applications e.g. drug discovery by simply replacing trypsin with newly invented drugs.

IV. TWO-DIMENSIONAL FLOW CHAMBER SPR IMAGING DETECTION SYSTEM

Another experiment is to monitor the specific binding of BSA antibody-antigen reaction in a 2-dimensional flow chamber array and a SPR imaging system. The microfluidic platform, which consists of two-dimensional flow chamber array, was fabricated by PDMS technique, as shown in Fig. 8. A silver layer (~500Å) was sputtered on a 60° equilateral prism (PH71 glass) and then covered with a gold protective layer (~50Å). The sensing layer was bonded to the PDMS microfluidic platform surface. The detection of specific BSA-anti-BSA binding in multi-chambers simultaneously was conducted. The process sequence is illustrated in Fig. 9. The sequence of injecting biovine serum albumin (BSA), phosphate-buffered saline (PBS), nonspecific

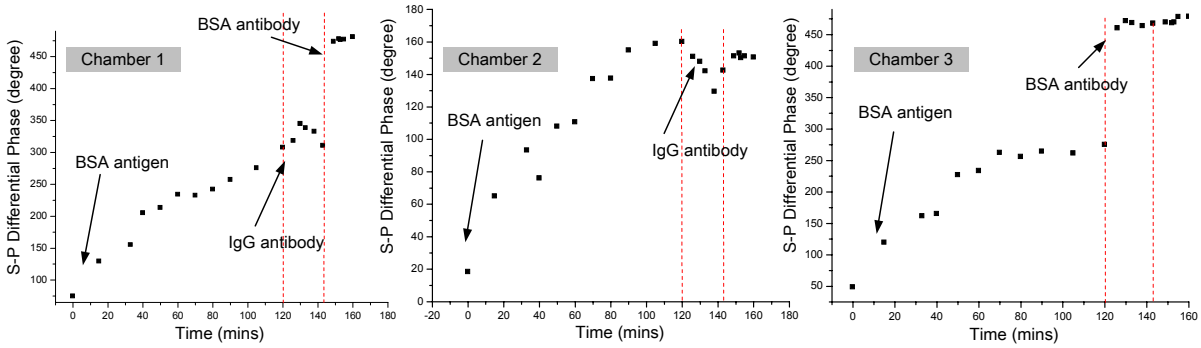

Fig. 10. Response curves of differential phase at different flow chambers after sequential addition of PBS, BSA, nonspecific BSA antibody (Rat IgG), and BSA antibody into the sensor head, demonstrating the detection of specific BSA-anti-BSA binding in multi-chambers simultaneously.

BSA antibody (Rat IgG), and BSA antibody into the sensor head is different from each chamber. Response curves of differential phase in different chambers can be monitored simultaneously. As shown in Fig. 10, the differential phase angle of all chambers increased upon the addition of BSA-molecules indicating the binding of BSA onto the sensor head surface. Then (at 120mins), chamber 1 and 2 were injected non-BSA antibodies (Rat IgG), and the differential phase angle remained constant, thus confirming that no nonspecific binding had taken place. At the same time, when chamber 3 was injected BSA specific antibodies, a sharp increase in phase angle was observed, indicating the binding reaction of BSA with the BSA antibodies. Afterward (at 142mins), chamber 1 was injected BSA specific antibodies, a sharp increase in phase angle was also observed.

In our future work, integrating the 2-dimensional detection chambers and the vortex micropumps into a single chip to become an automated detection system is an exciting direction. High throughput and automated multi9-chamber system for chemical and biological applications will provide a useful platform.

V. CONCLUSION

Monitoring of cell activities has been successfully demonstrated using our new SPR biosensor integrated with automated microfluidic system. This preliminary study on cell activity showed the possibilities of using differential phase SPR bio-sensors in a wide range of biomedical applications. Our integrated system should provide a useful platform for conducting high-throughput diagnostic tests on cells and biomolecules at a very low cost. Furthermore, arrayed sensing surface with multiple analytes and parallel detection by using a 2-dimensional phase imaging technique will certainly be a very exciting direction for further development of phase-sensitive SPR sensors.

ACKNOWLEDGEMENT

The authors wish to thank The Chinese University of Hong Kong for providing research studentships to W.C. Law. Funding support from a CUHK Direct grant under Project #2050305 and from a HKRGC Grant (CUHK 4215/01E) are also gratefully acknowledged.

REFERENCES

[1] D. J. Harrison, K. Fluri, K. Seiler, Z. Fan, C. S. Effenhauser and A. Manz, "Micromachining a Miniaturized Capillary Electrophoresis-based Chemical Analysis System on a Chip", *Science* 261, pp.895-897, 1993.

[2] M. J. Powers, K. Domansky, M. R. Kaazempur-Mofrad, A. Kalezi, A. Capitano, A. Upadhyaya, P. Kurzawski, K. E. Wack, D. B. Stolz, R. Kamm and L. G. Griffith, "A Microfabricated Array Bioreactor for Perfused 3D Liver Culture", *Biotechnol. Bioeng.* 78, pp.257-269, 2002.

[3] J. Melendez, R. Carr, D. U. Bartholomew, K. Kukanskis, J. Elkind, S. Yee, C. Furlong and R. Woodbury, "A commercial solution for surface plasmon sensing", *Sensors and Actuators*, B 35, pp.212-216, 1996.

[4] S. Y. Wu, H. P. Ho, W. C. Law, C. Lin and S. K. Kong, "Highly Sensitive Differential Phase-sensitive Surface Plasmon Resonance Biosensor Based on the Mach-Zehnder Configuration", *Optics Letters*, vol. 29, no. 20, pp.2378-2380, March 2004.

[5] K. F. Lei and Wen J. Li, "Microfluidic Mixing by Fluidic Discretization", accepted, *13th International Conference on Solid-State Sensors, Actuators, and Microsystems*, (*Transducers 2005),* Jun 05-09 2005, Korea.

[6] K. F. Lei, W. J. Li and Y. Yam, "Fabrication, Modeling, and Experimental Analysis of a Novel Vortex Micropump for Applications in PMMA-Based Micro Fluidic Systems", submitted, *Journal of Micromechanics and Microengineering*, Institute of Physics, U. K., 2005.

[7] P. Yeh, *Optical Waves in Layered Media*, Wiley, New York, 1988.

[8] Invitrogen Catalog, Invitrogen Corporation. www.invitrogen.com.